

Structural and electronic properties of narrow-gap ABC_2 chalcopyrite semiconductors

A. Continenza,* S. Massidda,[†] and A. J. Freeman

Department of Physics and Materials Research Center, Northwestern University, Evanston, Illinois 60208

T. M. de Pascale and F. Meloni

Dipartimento di Scienze Fisiche, Università di Cagliari, Cagliari, Italy

M. Serra

Istituto di Fisica Superiore, Università di Cagliari, Cagliari, Italy

(Received 4 March 1992)

The structural and electronic properties of some $A^{II}B^{IV}C_2^V$ ternary semiconductors with chalcopyrite structure are investigated using both the full potential linearized augmented plane wave and the *ab initio* pseudopotential methods. The total-energy approach is used to determine the internal distortion parameter u , discussed for these materials in terms of atomic radii. In addition, we study the band-gap anomaly, defined as the energy difference with respect to the III-V binary analog compound, and the crystal-field splitting of the valence-band maximum. We also present a total-energy study of the equilibrium structure of $CdSnSb_2$, a potential new chalcopyrite semiconductor that might be stabilized via epitaxial growth on the well-matched $InSb$ substrate.

I. INTRODUCTION

Ternary ABC_2 semiconductors which crystallize in the chalcopyrite structure¹ form a wide family of materials, which includes $A^I B^{III} C_2^{VI}$ and $A^{II} B^{IV} C_2^V$ type compounds. They have technological interest related to their nonlinear optical properties; for some of the $A^{II} B^{IV} C_2^V$ pnictide compounds ($A = Mg, Zn, Cd$; $B = Si, Ge, Sn$; and $C = P, As, Sb$), their narrow gaps make them suitable as infrared detectors. The larger degree of freedom with respect to that of their binary analogs provides a valid reason for interest in their possible device applications due to the wide variety of optical gaps offered by this class of materials.

The physical and chemical properties of ABC_2 semiconductors have been extensively studied in the last twenty years.¹⁻⁶ The chalcopyrite arrangement may be considered as a superlattice of the zinc-blende structure in which two kinds of cations cause the doubling of the unit cell along the c axis and each anion C is surrounded in a tetrahedral coordination by two cations of each type (A and B). Briefly, an $ABAB$ sequence is observed for the cations in the (001) and (110) directions, while along the (100) and (010) directions the sequence is AAA . As a consequence, the crystal shows a tetragonal distortion and a value of $\eta = c/2a$ usually smaller than unity. Also, the anion sublattice is distorted relative to the perfect fcc arrangement of the zinc-blende structure, producing different $A-C$ and $B-C$ bond lengths. This distortion is characterized by the internal parameter u , which is $\frac{1}{4}$ in the ideal (zinc-blende-like) structure. In particular, values of $u > \frac{1}{4}$ correspond to the anion being closer to the B than to the A cation (when the A cation is at the origin of the coordinates).

The combined effect of cation alternation and crystal-

lographic distortions makes the electronic energy bands of the ternary (e.g., $ZnGeP_2$) look different from the (folded) bands of the analog isoelectronic binary compound (e.g., GaP). In particular, the gap is usually smaller and a tetragonal crystal field Δ_{CF} splitting is induced at the valence-band maximum.

The problem of the structural and energy-gap anomalies (defined as the differences with respect to the binary analog compound) has received considerable interest both from the experimental and the theoretical point of view: a simple electrostatic scheme⁷ has been used to explain the $A-C$ and $B-C$ bond length differences and also the bond charge distribution. The structural parameters have been also discussed by Abrahams and Bernstein⁸ and by Van Vechten and Phillips.⁹ More recently an extensive self-consistent study by Jaffe and Zunger¹⁰ accounted in a very satisfactory way for the band-gap anomalies of the $A^I B^{III} C_2^{VI}$ crystals.

In this work, we focus our attention on the $A^{II} B^{IV} C_2^V$ compounds, and study their structural and electronic properties. As prototype members of this family we study $MgSiP_2$, $ZnSiP_2$, $ZnGeP_2$, $CdSiP_2$, $CdSnP_2$, and $CdSnAs_2$. This choice should provide a relatively general scenario of this class, since it includes both the case of isocore A and B cations, and the case of lighter B atoms. In addition, we study the ground-state equilibrium properties of the hypothetical chalcopyrite compound $CdSnSb_2$. There are several reasons why this material is interesting and looks promising: first of all, it is the only one of the series $CdSn = C_2$ ($C = P, As, Sb$) that does not exist in nature; second, its favorable matching conditions with $InSb$ (practically zero lattice mismatch, as we will show later) seem to indicate that it can be easily stabilized if grown via any epitaxial method; finally, it may represent a good candidate in the search for a crystalline

material with a narrow direct band gap (a band gap possibly smaller than InSb). The aim of the present study is to provide a systematic analysis of several different $A^{II}B^{IV}C_2^V$ chalcopyrite compounds in order to find more general trends that can help the understanding of their ground-state properties.

Our calculations are based on the local-density approximation (LDA) (Ref. 11) and use the full potential linearized augmented plane wave (FLAPW) (Ref. 12) and the *ab initio* pseudopotential¹³ methods. While the tetragonal distortion parameter η is precisely determined experimentally, the internal parameter u is only obtained in an indirect way. Therefore, the total-energy approach is needed to calculate the equilibrium u value. The total-energy approach is also used to determine all the equilibrium structural parameters of CdSnSb₂, since there are no experimental values that can be used to fix the value of the distortion parameter η and of the zinc-blende lattice parameter a .

In Sec. II we discuss the main points of the crystallographic structure and the computational methods used. In Sec. III we illustrate the results on the structural properties, while the electronic properties are compared with experiment in Sec. IV. Finally, in Sec. V we draw some conclusions.

II. STRUCTURE AND METHOD

The space group of the ternary ABC_2 chalcopyrite structure is D_{2d}^{21} . The unit cell contains two formula units (eight atoms) per unit cell, and the atomic positions are [in units of the lattice parameters (a, a, c)]: A $(0,0,0)$, $(0, \frac{1}{2}, \frac{1}{4})$; B $(\frac{1}{2}, \frac{1}{2}, 0)$, $(\frac{1}{2}, 0, \frac{1}{4})$; C $(u, \frac{1}{4}, \frac{1}{8})$, $(-u, \frac{3}{4}, \frac{1}{8})$, $(\frac{3}{4}, u, \frac{7}{8})$, $(\frac{1}{4}, -u, \frac{7}{8})$. In our calculations, we use the all-electron full potential linearized augmented plane wave (FLAPW) (Ref. 12) and the *ab initio* pseudopotential¹³ methods, with the local-density approximation (LDA) and with the Hedin and Lundqvist¹⁴ form for the exchange-correlation potential.

In the FLAPW calculations the core states are calculated fully relativistically and updated at each iteration, whereas for the valence states a semirelativistic calculation is performed; the effect of spin-orbit coupling on the energy bands is considered as a perturbation on the semirelativistic calculation. In the present calculation, the outermost d states of the group-II elements, as well as those of Ga and In, are considered as part of the valence bands, since they are quite shallow in energy (see discussion later). The Sn $4d$ orbitals, on the other hand, are considered as (self-consistently updated) core states, and the ~ 0.18 electrons spilling out of the muffin-tin sphere are treated by means of the overlapping charge method. Inside the muffin-tin spheres, the wave function is expanded in spherical harmonics up to $l_{\max}=8$, while $l_{\max}=6$ is used for the charge-density and potential expansions. Integrations over the irreducible wedge of the Brillouin zone were performed using four special \mathbf{k} points.¹⁵

In the calculations performed in the pseudopotential framework the electron-ion interaction is described via the *ab initio* norm-conserving pseudopotentials as deter-

mined by Bachelet, Hamann, and Schlüter.¹⁶ The input exchange-correlation potentials are those by Ceperley and Alder¹⁷ as interpolated by Perdew and Zunger.¹⁸ The Bloch states have been expanded into a plane-wave (PW) basis set, with the inclusion of plane waves with kinetic energy up to 14 Ry corresponding to ~ 1000 –1200 PW. A block version of Davidson's algorithm¹⁹ was employed to treat the eigenvalue problem. The \mathbf{k} -point mesh used for the Brillouin zone integrations was the same as in the FLAPW calculation.¹⁵

III. STRUCTURAL PROPERTIES

As previously pointed out, the chalcopyrite structure has three parameters (a , $\eta=c/2a$, and u) which accommodate the difference between the A and B cations. In particular, u is related to the A - C and B - C bond lengths (R_{AC} and R_{BC}) by the relations

$$R_{AC} = [u^2 + (1 + \eta^2)/16]^{1/2} a$$

and

$$R_{BC} = [(u - 1/2)^2 + (1 + \eta^2)/16]^{1/2} a .$$

Various attempts have been made so far to systematize these parameters for the chalcopyrites and the pnictides in particular. Hereafter, for sake of completeness, we shall mention some particular models. Folberth and Pfister²⁰ obtained qualitative agreement with experiment by assuming that $1 - \eta$ is related to the covalent and ionic character of the bonds. A correlation between $1 - \eta$ and a combination of bond orbital radii, proposed by Chelikowsky and Phillips,²¹ could account for the tetragonal distortions of the $A^{II}B^{IV}C_2^V$ chalcopyrites with the exception of CdSnP₂ and CdSnAs₂. As for the internal anion displacement u , only few models exist which try to explain its behavior. Among them, we mention Abrahams and Bernstein⁸ who proposed that the group-IV elements tend to conserve the tetrahedral bond angles. As a consequence, R_{AC} comes out to be larger than R_{BC} . However, while this argument could (at least partially) hold for the cases in which Si or Ge is the group-IV element, it is justified for Sn where the tendency to metallicity is more accentuated. Even for Si and Ge, however, bond-distance stretching is known to be energetically less favorable than bond bending. A systematic attempt to explain the structural coordinates of chalcopyrites has been made by Jaffe and Zunger.¹⁰ Starting from the principle of the conservation of the tetrahedral bond lengths (CTB), and using different sets of atomic radii, they were able to obtain good agreement with experiment. In particular, the set of radii by Shannon and Prewitt²² was shown to give the best overall results.

However, no first-principles theoretical calculation of these parameters has been reported so far. This is especially necessary in view of the fact that, as pointed out earlier, the determination of u is an indirect one (u is in fact obtained from crystallographic structural refinements related to several necessary starting assumptions^{1,8}). Since the electronic properties are strongly dependent on the u value, its determination from total-energy calculations is a necessary first step in the study of

these materials. The lattice constants a and c , on the other hand, are measured with good accuracy; we therefore use their experimental values in our calculations for all the compounds considered except for CdSnSb_2 . This, of course, allows us to avoid a costly multiparameter total-energy minimization that, however, cannot be avoided in the case of CdSnSb_2 for which no experimental results are available. As a test of our assumption, however, we calculated the a_{eq} and c_{eq} parameters for ZnSiAs_2 (keeping the u parameter fixed to its experimental equilibrium value), and obtained agreement with experiment to within about 0.1%. This approximation obviously implies a loss of accuracy in our determination of u ; however, since the equilibrium a and c values are obtained with very good accuracy, this should not be a serious handicap. Since the pseudopotential (PS) method is known to have problems in treating elements such as Zn and Cd due to the presence of shallow d levels, we only performed pseudopotential total-energy calculations on MgSiP_2 ; we obtained $u = 0.29$, in good agreement with the FLAPW results (see Table I).

The experimental^{10,23} and calculated values of the structural coordinate u are shown in Table I together with the lattice parameters obtained via a full total-energy minimization for the CdSnSb_2 . For this case, we found that the equilibrium volume is practically identical to that of the parent binary compound InSb ,²⁴ since the parameter a is equal, within our numerical accuracy, to the InSb zinc-blende lattice constant and the tetragonal distortion found is rather small ($\eta = 0.985$). This is not surprising and reflects the influence of atomic size on these compounds; chalcopyrite structures based on elements of the same row tend to keep the same volume as the related zinc blende since the alternate substitution of the cation with the group-II and group-IV elements is “self-compensating.” For CdSnP_2 (InP) and CdSnAs_2 (InAs) the difference between the a value in the binary and in the ternary compounds is in fact very small ($\sim 0.5\%$). This is also true for the Ge row: the ZnGeAs_2 chalcopyrite (not considered here) has almost the same volume¹⁰ as the parent GaAs zinc blende [very similar a and very small tetragonal distortion, $\eta = 0.983$ (Ref. 10)]. However, if we consider the row above, i.e., the Si row, we find that the volume of MgSiP_2 is

significantly different from twice the volume of the related zinc-blende AIP due to the higher difference in atomic size among Mg, Al, Si (see discussion later).

Several other remarks can be made based on the results shown in Table I. First of all, the agreement of our calculation with experiment is only qualitatively good, in contrast to the excellent agreement found for the *directly measured* a and c parameters for ZnSiAs_2 and for the binary compounds.^{24,25} The calculations in fact give a systematic deviation toward smaller values of u , corresponding to larger B - C distances. We have to note, however, that a large scattering between different experiments is observed for these and other chalcopyrites (see for instance Table II of Ref. 10). We note that when the A and B cations are isocore, the calculated u value is very close to the ideal value 0.25. The only significant deviations from the ideal structure are found in CdSnSb_2 , and are greater for MgSiP_2 and for the nonisocore compounds ZnSiAs_2 and CdSiP_2 . In the case of compounds containing Sn, we have to consider the fact that the equilibrium bond length of Sn is slightly overestimated by LDA calculations²⁶ and this can possibly explain the constant deviation toward a smaller value of u , with respect to experiment, in all the compounds containing Sn.

Related to the discussion of the equilibrium geometries, it is interesting to study the valence charge densities for some of these compounds. In Fig. 1(a) we show contour plots of the electronic valence charge density of CdSnP_2 , in a plane cutting the Cd-P-Sn bonds. The asymmetry of the bonds around P is evident. In order to show the chemical effects related to the cation alternation, we subtract from this charge distribution that corresponding to the binary analog InP , and plot the results in Fig. 1(b). The additional electron of Sn, in comparison to In, is mainly localized around the Sn nucleus, showing a relatively spherical charge distribution; the Cd atoms, on the other hand, show an electronic charge depletion relative to In which is more anisotropic than the accumulation around Sn. Very close to P, there is a tendency to screen the excess (deficiency) charge around Sn (Cd). It is interesting now to compare the CdSnP_2 charge density with that of CdSiP_2 plotted in Fig. 1(c) on the same plane. The Si atom shows, besides the smaller atomic size, a greater bond directionality compared to Sn. The charge on the Cd-P bonds, although slightly larger in CdSnP_2 , does not show any further relevant change. This is consistent with an almost identical bond length in the two different compounds as discussed below. The larger amount of charge observed on the Cd-P bond in CdSnP_2 is related to the less tightly bound nature of the Sn- $5p$ with respect to the Si- $3p$ electrons.

In order to discuss in more detail the structural coordinates, we list in Table II the calculated equilibrium distances together with the experimental results^{23,33–36} and with the predictions of various sets of atomic radii and of existing models. We notice that the Si compounds show a trend which may be related to Abrahams and Bernstein’s⁸ idea of preservation of tetrahedral angles. This model is, however, not verified for the other compounds studied, including the Ge compounds. It is well known that angles in tetrahedrally coordinated com-

TABLE I. Structural equilibrium parameters a , η , and u . All values are in angstroms.

	a	η	$u_{\text{expt.}}^a$	u
MgSiP_2	5.718	0.885	0.292	0.29
CdSnP_2	5.900	0.976	0.265	0.25
CdSnAs_2	6.094	0.978	0.261	0.25
CdSnSb_2	6.479 ^b	0.985 ^b		0.24
CdSiP_2	5.678	0.919	0.297	0.29
ZnGeP_2	5.465	0.985	0.267	0.25
			0.258	
ZnSiAs_2	5.610	0.970	0.266	0.26

^aValues taken from Table II of Ref. 10 and from Ref. 23.

^bValues calculated by a total-energy minimization using FLAPW.

pounds can be stretched easily as compared to bond lengths.

Interesting questions regarding the structural properties of these compounds are: (i) do bond lengths obey a simple additivity rule, as proposed by Jaffe and Zunger¹⁰

and, if so, (ii) which is the set of atomic radii, among those available in the literature, that explains better our first-principles findings? In order to better address these issues, we report in Table II the Pauling³¹ and Phillips and Van Vechten³² sets of radii among the many proposed so far. (The extensive work by Shannon and Prewitt²² considers radii obtained from sulfide compounds only, and therefore was not included in our list.) From an analysis of Table II, we notice that the Cd-P distance is well preserved upon going from CdSnP₂ to CdSiP₂, while the Si-P distance changes by $\approx 0.5\%$ from MgSiP₂ to CdSiP₂. Our calculations also seem to indicate that the atomic radii set of Phillips and Van Vechten gives better overall agreement with the first-principles results, as compared to the Pauling set. The main reason for this is that the Phillips and Van Vechten radii are equal when the group-II B and group-IV A cations belong to the same row of the periodic table. Our calculations in fact indicate that $u \approx 0.25$ in these cases.

We note also that MgSiP₂ has the same $u = 0.29$ value as CdSiP₂, and that the tetragonal distortion is larger in the latter compound. This is related to the absence of

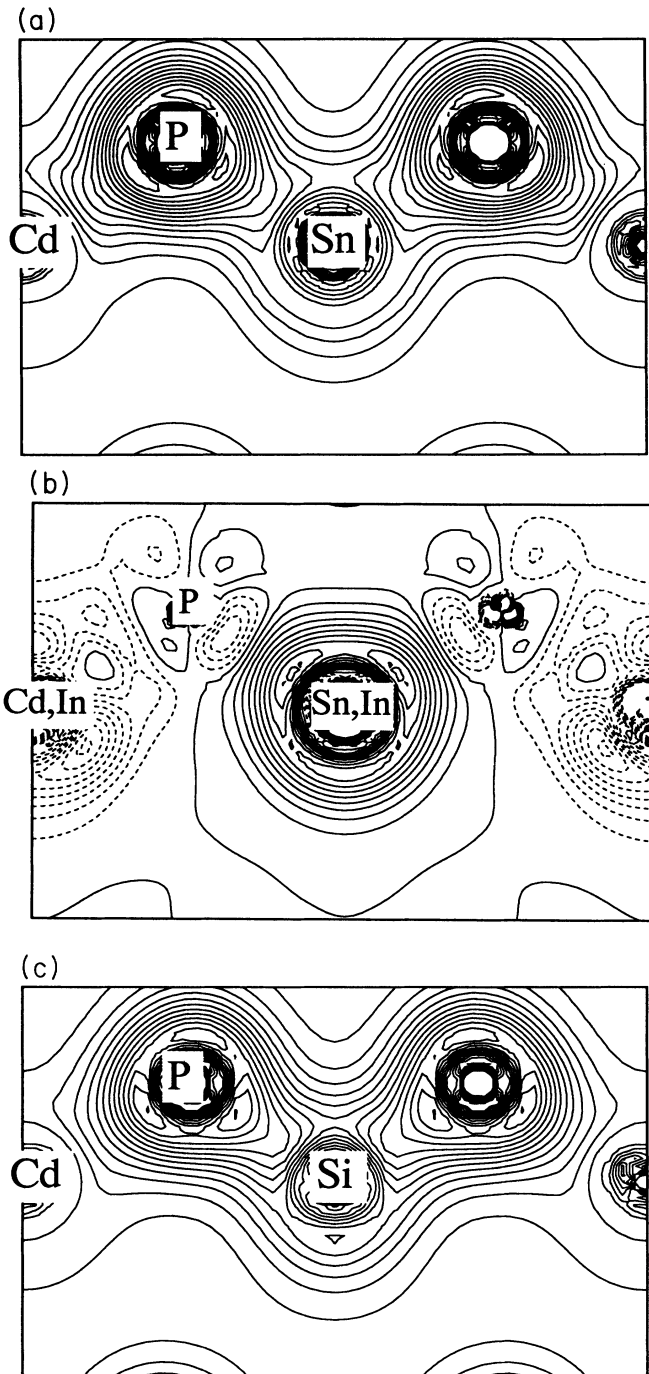


FIG. 1. (a) Total valence electron charge density of CdSnP₂ in a (110) plane; (b) difference between the above density and the valence electron density of InP with the same structural parameters of CdSnP₂ (dashed lines correspond to negative contours); (c) same as (a) for CdSiP₂. Levels are given in units of 10 electrons/cell [(a) and (c)] and 2 electrons/cell [(b)].

TABLE II. Experimental bond lengths in chalcopyrite compounds compared with Pauling (Ref. 31) and Phillips Van Vechten (Ref. 32) predicted values. The distances are in angstroms.

	Expt.	FLAPW	Pauling	PVV
Si-P	2.231 ^a	2.267 ^f	2.27	2.301
	2.247 ^b	2.255 ^g		
	2.248 ^a			
	2.249 ^a			
	2.254 ^c			
Ge-P	2.297 ^a	2.358	2.32	2.353
	2.308 ^d			
	2.323 ^e			
Si-As	2.345 ^a	2.373	2.35	2.398
	2.351 ^e			
Zn-P	2.373 ^c	2.352	2.41	2.353
	2.375 ^e			
	2.380 ^a			
	2.397 ^d			
	2.405 ^a			
Zn-As	2.453 ^e	2.431	2.49	2.450
	2.469 ^a			
Sn-P	2.484 ^a	2.538 ^h	2.50	2.533
Mg-P	2.536 ^a	2.529 ^g		2.429
Sn-As	2.578 ^a	2.627	2.58	2.630
	2.583 ^d			
Sn-Sb		2.822 ⁱ	2.76	2.810
Cd-P	2.561 ^b	2.531 ^h	2.58	2.533
	2.580 ^a	2.536 ^f		
	2.587 ^a			
Cd-As	2.660 ^d	2.611 ^j	2.66	2.630
	2.663 ^a			
Cd-Sb		2.762 ⁱ	2.84	2.810

^aReference 23.

^bReference 33.

^cReference 34.

^dReference 35.

^eReference 36.

^fCdSiP₂.

^gMgSiP₂.

^hCdSnP₂.

ⁱCdSnSb₂.

^jCdSnAs₂.

semicore d levels in Mg, which makes its atomic size comparable with that of Cd and larger than that of Zn, where the $3d$ states do not screen completely the corresponding nuclear charge as seen by the valence s states (the tetragonal distortion in ZnSiP_2 is, in fact, much smaller).

IV. ELECTRONIC PROPERTIES

In order to describe the general features of the bonding in these compounds, we show in Fig. 2 the total and muffin-tin projected partial density of states (PDOS) for CdSnP_2 . The lower band at around -12 to -10 eV is derived from the anion s states; at ~ -8 eV we find the Cd $4d$ orbitals, which form a relatively narrow band of ~ 1 -eV bandwidth, combining with a Sn s -derived band. The bands at higher energy, between -5 eV and the valence-band maximum (VBM), are mostly derived from the P p states, hybridized with the Cd and Sn p states. Direct hybridization between Cd and Sn states does not seem to be very strong, and can be seen for the s states in the region from -7 to -3 eV. We notice in Fig. 2 that at energies close to the VBM the Cd d states give a large contribution, comparable to that of Cd and Sn p . It was pointed out by Jaffe and Zunger¹⁰ for the $A^{\text{I}}B^{\text{III}}C_2^{\text{VI}}$ compounds that the p - d hybridization at the VBM gives a contribution to the band-gap anomaly. For the $A^{\text{II}}B^{\text{IV}}C_2^{\text{V}}$ compounds of interest here, this effect is expected to be smaller, and arises from the difference between the Cd $4d$ states and the In $4d$ states of the analog compound InP (see discussion later). The lower-lying conduction states are mainly due to Sn s states, with a noticeable hybridization with the P states (mostly p).

Figure 3 shows the energy bands of CdSnP_2 superimposed on those of its binary analog InP for an energy range close to the valence-band maximum. We note that

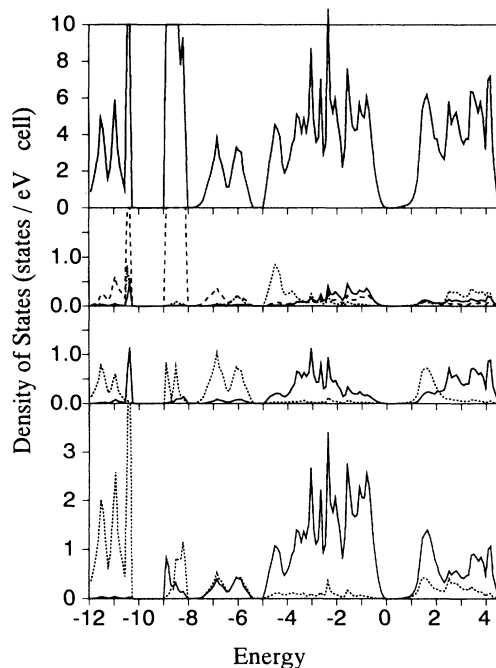


FIG. 2. Total and muffin-tin projected partial density of states for CdSnP_2 .

the energy gap is smaller in the ternary, and that the threefold Γ_{15} states are split by the tetragonal distortion into the twofold Γ_5 and the nondegenerate Γ_4 representations of the D_{2d} point group. These two effects, namely the band-gap anomaly and the crystal-field splitting, will be studied in detail in the following.

In Table III we list the minimum-energy-band gaps, including spin-orbit effects, of the chalcopyrite compounds studied, together with the experimental values and with the LDA gaps of the binary analog (when the A and B elements do not belong to the same row of the periodic table, we list the experimental gaps of the alloy $X_{0.5}Y_{0.5}C$ and the calculated LDA gaps of XC and YC , where X and Y are the group-III elements contiguous to A and B , respectively). All the chalcopyrites considered show a direct energy-band gap, whereas some of the binary analogs (AlP, GaP, and AlAs) show indirect band gaps (between the Γ - X , Γ - Λ , and Γ - X points, respectively) which become direct in the ternary structures, because of band-folding effects. Despite the disagreement with the experimental data due to the well-known inability of the local-density approximation to produce satisfactory values for the excited states of semiconductors, the energy-gap variations related to structural and possibly chemical changes may be expected to be well reproduced. Therefore, we shall investigate what are the ingredients that, according to our calculations, give rise to the band-gap anomalies in the $A^{\text{II}}B^{\text{IV}}C_2^{\text{V}}$ compounds illustrated in Table III.

To this aim, we choose CdSnP_2 as a first example, and we go from the binary to the ternary chalcopyrite compound by first imposing on InP the same tetragonal structure of CdSnP_2 [we recall that no internal anion distortion is found according to our total-energy calculations, and that $\eta=0.976$ (see Table I)]; then we introduce the cation alternation. The first step, which gives the contribution of the tetragonal distortion to the band-gap anomaly, is seen to produce a negative change of -0.02 eV in the direct band gap, while the second step gives a chemical term, which is seen to be -0.29 eV. The chemical

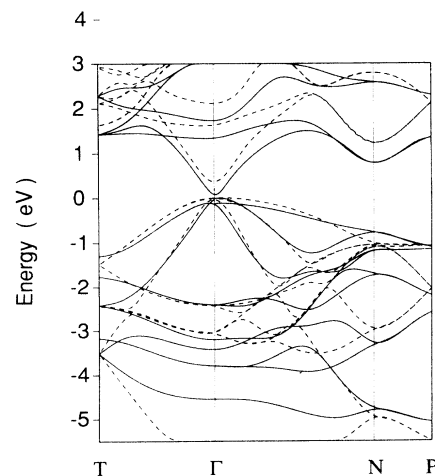


FIG. 3. Electronic energy bands of CdSnP_2 (full lines) and of InP (dashed lines) calculated with the chalcopyrite structure but with the zinc-blende parameters ($u=0.25, \eta=1$) along the main symmetry directions of the tetragonal Brillouin zone.

TABLE III. Minimum energy-band gaps compared with the experiments. The experimental band gaps of the binary or alloy analog compounds (XYC) have been added for comparison (see text). In the case of alloys, the theoretical values shown refer to the related binaries. The calculations are performed with the FLAPW method, including spin-orbit effects, unless differently indicated. All the band-gap values shown are direct band gap with the exception of AlP, GaP, and AlAs (the minimum band gap in these cases is between the Γ - X , Γ - A , and Γ - X points, respectively).

	Theory	Expt.	XYC	Theory	Expt.
MgSiP ₂	1.16 1.27 ^a		AlP	1.42	2.5 ^b
CdSnP ₂	0.03	1.17	InP	0.42	1.42 ^c
CdSnAs ₂	-0.72	0.26	InAs	-0.51	0.42 ^d
CdSnSb ₂	-0.80		InSb	-0.74	0.23 ^e
CdSiP ₂	1.16	2.2	In _{0.5} Al _{0.5} P	InP 0.42 AlP 1.42	2.16 ^c 2.5 ^b
ZnGeP ₂	1.07	2.2	GaP	1.42	2.87 ^f
ZnSiAs ₂	0.89	1.7	Ga _{0.5} Al _{0.5} As	GaAs 0.23 AlAs 1.37	2.11 ^{g,h} 2.22 ^b

^aPresent semirelativistic pseudopotential calculation.

^bReference 43.

^cReference 40.

^dReference 41.

^eReference 42.

^fReference 38.

^gReference 37.

^hReference 39.

term, therefore, represents the main contribution to the band-gap anomaly in this material. Jaffe and Zunger¹⁰ pointed out the contribution of the p - d hybridization to the band-gap anomaly of the $A^I B^{III} C_2^{VI}$ chalcopyrite compounds. In the case of the $A^{II} B^{IV} C_2^{V}$ materials however, this contribution may be expected to be smaller. In fact, going (for instance) from ZnS to CuGaS₂ means substituting the localized Zn 3*d* states with the bandlike Cu 3*d* states which, as shown by Jaffe and Zunger,¹⁰ are located at energies close to the valence-band maximum (-4 eV in CuInSe₂). On the other hand, although substituting the In 4*d* with the Cd 4*d* states in going from InP to CdSnP₂ implies a change in the same direction, the Cd 4*d* states are nevertheless located at binding energies around -8.5 eV relative to the valence-band maximum (within LDA) and their hybridization with the valence-band top is therefore expected to be smaller. In order to have a quantitative estimate of this effect, we performed FLAPW band calculations for InP and CdSnP₂ in which the *d* energy parameters of In and Cd are fixed to a very high value, so as to eliminate the corresponding component from the calculated eigenfunctions. The energy gaps change by 0.14 and ~0.16 eV, respectively, for the binary and ternary compounds, thereby providing a (rough) estimate of ~0.03 eV for the contribution of the p - d hybridization to the band-gap anomaly. Therefore, for CdSnP₂, we conclude that the chemical alternation effect is mainly responsible for the gap anomaly, and that only a relatively small fraction of this effect is due to p - d hybridization.

In considering the band-gap anomaly, one should also take into account the spin-orbit interaction that may, in principle, vary in going from the binary to the ternary compound because of the different p - d hybridization con-

tributions to the valence-band maximum. We have checked this point and compared the spin-orbit effect on the band-gap values for all the chalcopyrites and binaries used as references in Table III. In particular, we found that in all the structures considered, the relativistic contributions to the band-gap anomaly can be neglected since the spin-orbit splitting of the ternaries is essentially equal to that of the analog binaries (within ≤ 0.03 eV but typically ≈ 0.01 eV). This can also be regarded as an indirect confirmation of the small effect of the p - d hybridization (the only ingredient that may significantly change the spin-orbit splitting in the ternary relative to the binary) on the band-gap anomaly.

The effect of the cation ordering on the band gap for a fixed structure can be studied by using the virtual-crystal approximation, namely by comparing the disordered alloy Mg_{0.5}Si_{0.5}P with the ordered MgSiP₂ compound, both in the ideal structure. This is done by use of the pseudopotential method. The direct energy gap goes from 1.27 eV in the real crystal (with $u=0.29$) to 0.93 eV in the ideal structure and changes by less than 0.01 eV with that cation disorder (i.e., going to the virtual crystal). It appears, at least in this case, that the cation ordering itself is not important in determining the band gap when artificially separated by any structural effect. (We note that the value 1.27 eV found in the pseudopotential calculation agrees to within 0.1 eV with the FLAPW calculation.)

In order to examine the effect of the internal anion displacement on the band gap of these materials, we study it by the FLAPW method in MgSiP₂, where u is significantly greater than the ideal value. Going from $u=0.25$ to $u=0.29$ (the calculated equilibrium value), the gap changes from 0.93 to 1.17 eV. The change of

band gap due to the anion displacement is relatively large. In particular, since the band gap is related to the distance in energy between the anion p states and the Si s states, the increase of the internal distortion u (and the consequent decrease of the Si-P bond length) pushes up in energy the antibonding Si s states, thereby increasing the band gap. Similar trends are found in the case of the $A^I B^{III} C_2^{VI}$ compounds [such as CuInSe_2 (Ref. 10) where, however, we have an additional mechanism related to the covalent bonding with the filled d shells]. These states are in fact in the valence-band energy region and their hybridization with the anion p states pushes the valence-band maximum up in energy, therefore reducing the gap. An increase of the Cu-Se bond length associated with a larger u produces a reduction of the bond strength and a consequent band-gap opening. This additional mechanism explains the larger band-gap anomaly in the $A^I B^{III} C_2^{VI}$ chalcopyrites with respect to the $A^{II} B^{IV} C_2^V$. We notice that when the internal distortion u is smaller than the ideal value (0.25) it gives a positive contribution to the band-gap anomaly. In most of the $A^{II} B^{IV} C_2^V$ compounds, however, the anion displacement $u > \frac{1}{4}$ so that it acts as to reduce the anomaly, which is therefore a balance of the chemical and structural contributions. We therefore see a negative anomaly in CdSiP_2 , as a result of the large anion displacement overcoming the chemical contribution.

We report in Table III the band gap of the new compound CdSnSb_2 in the semirelativistic approximation and, also, including the spin-orbit effect as a perturbation on the semirelativistic results. The band gap of this compound is direct at the zone center and the band-gap anomaly, which in this case is dominated by the contribution of cation alternation (the structural distortions being relatively small), is quite small (≈ 0.06 eV). According to our prediction of the gap anomaly and considering that the experimental gap of InSb is 0.24 eV, the direct band gap of CdSnSb_2 should be 0.16 eV. Due to the tetragonal distortion of the chalcopyrite structure, the states at the valence-band maximum, Γ_{15} , are split into the two irreducible representations Γ_4 and Γ_5 of the D_{2d} point group. This splitting affects the VBM effective masses and therefore the conduction properties of these materials. It is therefore interesting to study this in detail in order to evaluate the importance of the correlation between Δ_{CF} and structural parameters. In Table IV we list our calculated values of the Δ_{CF} splittings and compare them with the experimental^{27–30} values. The agreement is satisfactory, the larger deviation being found in CdSnAs_2 . The

TABLE IV. Crystal-field splittings.

	FLAPW	Expt.
MgSiP_2	0.33	
CdSnP_2	0.12	0.10
CdSnAs_2	0.11	0.06
CdSnSb_2	0.10	
CdSiP_2	0.32	
ZnGeP_2	0.08	0.08
ZnSiAs_2	0.15	0.13

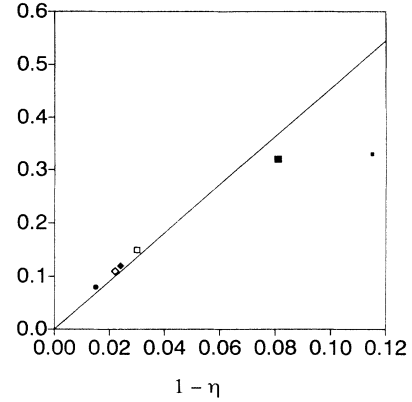


FIG. 4. Crystal-field splittings in ABC_2 chalcopyrites, plotted against the tetragonal distortion. The symbols are as follows: full and open symbols correspond to the anion being P and As, respectively; squares, circles, and triangles mean that the B cation is Si, Ge, and Sn, respectively, and finally the increasing size of the symbol indicates that the A cation is Mg, Zn, and Cd, respectively. The straight line connects the origin to a result obtained for InP in the chalcopyrite structure with the same tetragonal distortion as CdSnP_2 .

calculated values are plotted in Fig. 4 against $1 - \eta$. Apart from MgSiP_2 , the data show a linear behavior, which indicates that the tetragonal distortion is the main factor which determines Δ_{CF} . This is confirmed by a calculation performed on InP with the same tetragonal distortion of CdSnP_2 : the resulting $\Delta_{\text{CF}} = 0.1$ eV is very similar to the value of 0.11 eV found for the CdSnP_2 compound (the continuous line in Fig. 4 goes through this point). On the contrary, we notice a weak correlation between the crystal-field splittings and the internal distortion u , with the exception of MgSiP_2 , where the large internal distortion has some influence on Δ_{CF} .

V. CONCLUSIONS

We have studied some $A^{II} B^{IV} C_2^V$ chalcopyrite compounds using the FLAPW method and norm-conserving pseudopotentials. The total-energy approach was used to calculate the internal anion displacement u , which is determined only in an indirect way by the experiments. Our results show that u is nearly equal to its equilibrium value when the group-II and group-IV cations belong to the same row of the periodic table. An additivity rule for the atomic radii holds for the examples studied, and among the possible choices of atomic radii those of Van Vechten and Phillips seem to agree better with our results. The different contributions to the band-gap anomaly have been analyzed, leading to the following conclusions: the chemical effect (cation alternation) gives the strongest contribution (namely 0.29 eV, leading to a smaller gap in CdSnP_2) to the anomaly for those chalcopyrites where the u distortion is small. When u deviates strongly from the ideal value 0.25, however, it also contributes strongly (by 0.35 eV for MgSiP_2) to the gap anomaly. In particular, we found that the gap decreases when u increases.

ACKNOWLEDGMENTS

The work at Northwestern University was supported by the U.S. National Science Foundation (through the Northwestern University Material Research Center, Grant No. DMR 88-21571) and by a computing grant

from its Division of Advance Scientific Computing at the National Center for Supercomputing Application, University of Illinois, Champaign-Urbana. The work at Università degli Studi di Cagliari was supported by the Italian Consiglio Nazionale delle Ricerche CNR (through Progetto Finalizzato, Grant No. 89-00006-69).

*Present address: Dipartimento di Fisica dell'Università degli Studi di L'Aquila, I-67010 Coppito, Italy.

† Present address: Centro di Ricerca, Sviluppo e Studi Superiori in Sardegna, POB 488, I-09100 Cagliari, Italy

¹J. L. Shay and J. H. Wernick, *Ternary Chalcopyrite Semiconductors: Growth, Electronic Properties, and Applications* (Pergamon, New York, 1975).

²*Ternary Compounds 1977*, edited by D. G. Holah, IOP Conf. Proc. No. 35 (Institute of Physics, Bristol, 1977).

³Jpn. J. Appl. Phys. **19**, 1 (1980).

⁴Nuovo Cimento D **2**, 1609 (1983).

⁵Prog. Cryst. Growth Charact. **10**, 10 (1985).

⁶*Ternary and Multinary Compounds* (Materials Research Society, Pittsburgh, 1987).

⁷A. Baldereschi, F. Meloni, and M. Serra, *Il Nuovo Cimento D* **2**, 1643 (1983).

⁸C. Abrahams and J. L. Bernstein, *J. Chem. Phys.* **59**, 5415 (1973).

⁹J. A. van Vechten and J. C. Phillips, *Phys. Rev. B* **2**, 2160 (1970).

¹⁰J. E. Jaffe and A. Zunger, *Phys. Rev. B* **29**, 1882 (1984).

¹¹W. Kohn and P. Washista, in *Theory of the Inhomogeneous Electron Gas*, edited by S. Lundqvist and N. H. March (Plenum, New York, 1983).

¹²H. J. F. Jansen and A. J. Freeman, *Phys. Rev. B* **30**, 561 (1984).

¹³D. R. Hamann, M. Schlüter, and C. Chiang, *Phys. Rev. Lett.* **43**, 1494 (1979).

¹⁴L. Hedin and B. I. Lundqvist, *J. Phys. C* **4**, 2064 (1971).

¹⁵H. J. Monkhorst and J. P. Pack, *Phys. Rev. B* **13**, 5188 (1976); A. Baldereschi, *ibid.* **7**, 5212 (1973); D. J. Chadi and M. L. Cohen, *ibid.* **8**, 5747 (1973).

¹⁶G. B. Bachelet, D. R. Hamann, and M. Schlüter, *Phys. Rev. B* **26**, 4199 (1982).

¹⁷D. M. Ceperley and B. J. Alder, *Phys. Rev. Lett.* **45**, 566 (1980).

¹⁸J. Perdew and A. Zunger, *Phys. Rev. B* **23**, 5048 (1981).

¹⁹E. Davidson, in *Methods in Computational Molecular Physics*, edited by G. H. F. Dierkesen and S. Wilson (Reidel, Dordrecht, 1983).

²⁰O. G. Folberth and H. Pfister, *Acta Crystallogr.* **13**, 199 (1960).

²¹J. R. Chelikowsky and J. C. Phillips, *Phys. Rev. B* **17**, 2453

(1978).

²²R. D. Shannon, in *Structure and Bonding in Crystals*, edited by M. O'Keefe and A. Navrotsky (Academic, New York, 1981), Vol. II, p. 53.

²³A. A. Vaipolin, *Fiz. Tverd. Tela.* **15**, 1430 (1973) [*Sov. Phys Solid State* **15**, 965 (1973)].

²⁴S. Massidda, A. Continenza, A. J. Freeman, T. M. de Pascale, F. Meloni, and M. Serra, *Phys. Rev. B* **41**, 12079 (1990).

²⁵B. I. Min, S. Massidda, and A. J. Freeman, *Phys. Rev. B* **38**, 1970 (1988).

²⁶A. Continenza and A. J. Freeman, *Phys. Rev. B* **43**, 8951 (1991).

²⁷J. L. Shay, E. Buehler, and J. H. Wernick, *Phys. Rev. Lett.* **24**, 1301 (1970).

²⁸J. L. Shay, E. Buehler, and J. H. Wernick, *Phys. Rev. B* **2**, 4104 (1970).

²⁹J. L. Shay, E. Buehler, and J. H. Wernick, *Phys. Rev. Lett.* **30**, 983 (1973).

³⁰J. L. Shay, B. Tell, E. Buehler, and J. H. Wernick, *Phys. Rev. B* **3**, 2004 (1971).

³¹L. Pauling, *The Nature of the Chemical Bond* (Cornell University Press, Ithaca, 1967), p. 246.

³²J. A. Van Vechten and J. C. Phillips, *Phys. Rev. B* **2**, 2160 (1970).

³³S. C. Abrahams and J. L. Bernstein, *J. Chem. Phys.* **55**, 796 (1971).

³⁴S. C. Abrahams and J. L. Bernstein, *J. Chem. Phys.* **52**, 5607 (1970).

³⁵B. R. Pamplin, T. Kiyosawa, and K. Masumoto, *Prog. Cryst. Growth Charact.* **1**, 331 (1970).

³⁶M. D. Lind and R. W. Grant, *J. Chem. Phys.* **58**, 357 (1973).

³⁷R. Dingle, W. Wiegmann, and C. H. Henry, *Phys. Rev. Lett.* **33**, 827 (1974).

³⁸P. J. Dean, G. Kaminsky, and R. B. Zettersirom, *J. Appl. Phys.* **38**, 3551 (1967).

³⁹M. Sturge, *Phys. Rev.* **127**, 768 (1962).

⁴⁰W. J. Turner, W. E. Reese, and G. D. Pettit, *Phys. Rev.* **136**, A1467 (1964).

⁴¹C. R. Pidgeon, D. L. Mitchell, and R. N. Brown, *Phys. Rev.* **154**, 737 (1967).

⁴²E. J. Johnson, *Phys. Rev. Lett.* **19**, 352 (1967).

⁴³B. Monemar, *Phys. Rev. B* **8**, 5711 (1973).